HHS Public Access

Author manuscript

Neuropharmacology. Author manuscript; available in PMC 2018 April 01.

Published in final edited form as:

Neuropharmacology. 2017 April ; 116: 371–386. doi:10.1016/j.neuropharm.2017.01.010.

Modulation of neuroinflammation and pathology in the 5XFAD mouse model of Alzheimer's Disease using a biased and selective beta-1 adrenergic receptor partial agonist

Pooneh Memar Ardestani[a,#], **Andrew K. Evans**[a,#], **Bitna Yi**[a], **Tiffany Nguyen**[a], **Laurence Coutellier**[a,1], and **Mehrdad Shamloo**[a,*]

[a]Stanford University School of Medicine, Department of Neurosurgery, 1050 Arastradero Road, Building A, Palo Alto, CA 94304, USA

Abstract

Degeneration of noradrenergic neurons occurs at an early stage of Alzheimer's Disease (AD). The noradrenergic system regulates arousal and learning and memory, and has been implicated in regulating neuroinflammation. Loss of noradrenergic tone may underlie AD progression at many levels. We have previously shown that acute administration of a partial agonist of the beta-1 adrenergic receptor (ADRB1), xamoterol, restores behavioral deficits in a mouse model of AD. The current studies examined the effects of chronic low dose xamoterol on neuroinflammation, pathology, and behavior in the pathologically aggressive 5XFAD transgenic mouse model of AD. *In vitro* experiments in cells expressing human beta adrenergic receptors demonstrate that xamoterol is highly selective for ADRB1 and functionally biased for the cAMP over the β-arrestin pathway. Data demonstrate ADRB1-mediated attenuation of TNF-α production with xamoterol in primary rat microglia culture following LPS challenge. Finally, two independent cohorts of 5XFAD and control mice were administered xamoterol from approximately 4.0–6.5 or 7.0–9.5 months, were tested in an array of behavioral tasks, and brains were examined for evidence of neuroinflammation, and amyloid beta and tau pathology. Xamoterol reduced mRNA expression of neuroinflammatory markers (Iba1, CD74, CD14 and TGFβ) and immunohistochemical evidence for microgliosis and astrogliosis. Xamoterol reduced amyloid beta and tau pathology as measured by regional immunohistochemistry. Behavioral deficits were not observed for 5XFAD mice. In

[*]Corresponding Author: Mehrdad Shamloo, Stanford University School of Medicine, Department of Neurosurgery, 1050 Arastradero Road, Building A, Palo Alto, CA 94304. Tel: (650) 725-3152; Fax: (650) 723-4147; mshamloo@stanford.edu.

[1]Present address: Ohio State University, Departments of Psychology & Neuroscience

[#]Indication of co-first author status

Chemical Compounds studied in this article

xamoterol (PubChem CID: 155774);
isoproterenol (PubChem CID: 3779);
betaxolol hydrochloride (PubChem CID: 107952)
CGP 20712A (PubChem CID: 2685)
ICI-118551 (PubChem CID: 5484725)

Conflicts of Interest

Cortice Biosciences has licensed a patent for xamoterol from Stanford University. MS previously served as a paid scientific advisor for Cortice until May 2016. This work was not designed, initiated or funded by Cortice.

conclusion, chronic administration of a selective, functionally biased, partial agonist of ADRB1 is effective in reducing neuroinflammation and amyloid beta and tau pathology in the 5XFAD model of AD.

Keywords

Alzheimer's Disease; neuroinflammation; amyloid beta; xamoterol; beta-1 adrenergic receptor; 5XFAD

1. Introduction

Alzheimer's Disease (AD) is defined by amyloid beta and tau pathology, neurodegeneration, neuroinflammation, and cognitive dysfunction. Neuroinflammation is both a contributing factor to and a consequence of neurodegeneration and contributes to cognitive dysfunction (Cunningham et al. 2009; Sil and Ghosh 2016; Singhal et al. 2014). It has been suggested that chronic inflammation in response to neuronal damage may accelerate and potentially underlie disease progression in AD, with resident microglia being a key player involved in neuronal and synaptic loss. On the other hand, monocyte-derived macrophages are thought to be recruited to sites of neurodegeneration where they may play a beneficial role in suppressing neuroinflammation, and repairing damage (Schwartz and Shechter 2010; Koronyo-Hamaoui et al. 2009; Rezai-Zadeh et al. 2011). While the regulatory mechanisms and function of neuroinflammation in AD are not well-understood, genome wide association studies have repeatedly identified immune-related pathways as a source of primary susceptibility in AD, warranting further investigation (Lambert et al. 2010).

Degeneration of locus coeruleus (LC), the primary source of forebrain projecting noradrenaline (NA) neurons, may contribute to both cognitive deficits and neuroinflammation in AD (Mather and Harley 2016; Ross et al. 2015). The LC is one of the first sites of pathology in AD (Braak et al. 2011) and loss of NA neurons in the LC (German et al. 1992; Bondareff et al. 1987; Matthews et al. 2002), decreased NA in cortical and limbic projection regions (Matthews et al. 2002), and changes in post-synaptic NA receptors (Shimohama et al. 1987; Kalaria et al. 1989), and transporters (Tejani-Butt et al. 1993) have all been reported in AD. The extent of LC degeneration has been shown to be positively correlated to both cognitive deficits and pathology (Bondareff et al. 1987; Matthews et al. 2002) in humans, and this has been supported in numerous experimental models of AD.

Multiple lines of evidence indicate that experimental reduction of NA tone exacerbates AD-related pathology and cognitive deficits in transgenic mouse models of AD (Heneka et al. 2010). Pharmacological lesion of NA neurons in the LC in transgenic mice overexpressing human amyloid beta protein precursor (AβPP) results in elevated amyloid beta plaque load, increased neuronal loss, elevated markers of inflammation, impaired migration of microglia to plaque sites, impaired microglial phagocytosis of amyloid beta, and deficits in social and spatial memory tasks (Heneka et al. 2006; Heneka et al. 2010; Kalinin et al. 2007). Many of these deficits are reversed with NA or NA precursor supplementation. Additionally, pharmacological blockade of beta-adrenergic receptors in a mouse model of AD has been

shown to exacerbate cognitive deficits and neuroinflammation and to increase amyloid beta and plaque loads (Branca et al. 2014).

While lack of adrenergic tone on neuronal receptors likely contribute to AD-related cognitive deficits, given the role of NA in arousal and learning and memory (Thomas 2015), adrenergic receptors on microglia and astrocytes are also likely to contribute to AD-related disease progression. Adrenergic receptors on microglia and astrocytes have been shown to modulate cytokine release, microglia phagocytosis, and release of growth and proliferation factors, contributing protective mechanisms for neuronal function and survival (Madrigal et al. 2009; Madrigal et al. 2005; Fujita et al. 1998; Yang et al. 2012; Markus et al. 2010; Suryono et al. 2006). Neurons, microglia, and astrocytes express beta1 and beta2 adrenergic receptors (ADRB1 and ADRB2) (Tanaka et al. 2002; Day et al. 2014; Murchison et al. 2011; Schutsky et al. 2011a; Mori et al. 2002). NA has a higher affinity for the ADRB1 receptor relative to the ADRB2 receptor (Bylund et al. 1994; Tanaka et al. 2002) but both are engaged across a range of physiologically relevant contexts (Schutsky et al. 2011a). The specific role of adrenergic receptor subtypes in modulation of AD-related neuroinflammation, pathology and cognitive deficits has not been well-characterized or has been characterized with non-selective pharmacology.

We have previously demonstrated that acute treatment with a selective partial agonist of the ADRB1 receptor, xamoterol, can restore behavioral deficits in a mouse model of Down's Syndrome (Faizi et al. 2011) and in transgenic mice overexpressing human AβPP (Coutellier et al. 2014). Rescue of cognitive function with acute activation of ADRB1 via xamoterol likely involves the PKA/cAMP pCREB signaling cascade (Coutellier et al. 2014). The current studies were designed to determine the effects of chronic administration of the selective and partial agonist of the ADRB1 receptor, xamoterol, on AD-related pathology, neuroinflammation, and behavior in a 5XFAD transgenic mouse model of AD in early and late stages of disease pathology. We first demonstrate that xamoterol is a highly selective partial agonist at the ADRB1 receptor with functional bias for the cAMP pathway over the β-arrestin pathway. We then demonstrate anti-inflammatory effects on TNF-α production in rat primary microglia culture. Finally, *in vivo* studies in the 5XFAD transgenic mouse model of AD demonstrate that chronic administration of xamoterol leads to changes in pathological features of disease progression including attenuation of neuroinflammation across both early and late stages of disease pathology and reduction of amyloid beta and tau pathology.

2. Materials and Methods

2.1. Xamoterol pharmacology

2.1.1. cAMP assay—ADRB receptor subtype-mediated effects of xamoterol at the cAMP pathway were evaluated by measuring cAMP production using the homogenous time-resolved fluorescence detection method. Agonist activity of xamoterol at ADRB1, ADRB2, and ADRB3 were measured using HEK-293 cell stably expressing human recombinant ADRB1, CHO cells stably expressing human recombinant ADRB2, and human SK-N-MC neurotumor cells endogenously expressing ADRB3. Briefly, cells were suspended in HBSS buffer completed with 20 mM HEPES (pH 7.4) and 500 μM IBMX (3-isobutyl-1-methylxanthine) and distributed at a density of $3x10^3$ cells/well (HEK-293 cells) or 10^4

cells/well (CHO cells and SK-N-MC cells). Subsequently, cells were incubated with HBSS (basal control), the full agonist isoproterenol (Sigma-Aldrich, I5627), or xamoterol (S-enantiomer; Santai Pharmaceuticals) for 30 min (HEK-293 cells and CHO cells) or 10 min (SK-N-MC cells). Following incubation, the cells were lysed and the fluorescence acceptor (D2-labeled cAMP) and fluorescence donor (anti-cAMP antibody labeled with europium cryptate) were added. After 60 min incubation with the fluorescence donor and acceptor at room temperature, the fluorescence transfer was measured at 337 nm (excitation) and 620 and 665 nm (emission) using a microplate reader. The cAMP concentration was determined by dividing the signal measured at 665 nm by that measured at 620 nm (ratio). The results were expressed as a percent of the maximum efficacy achieved with isoproterenol.

2.1.2. β-arrestin assay—Effects of xamoterol at the β-arrestin pathway mediated by ADRB1 and ADRB2 were evaluated using enzyme fragment complementation method with β-galactosidase as the functional reporter. Agonist activity of xamoterol at ADRB1 and ADRB2 were measured using engineered CHO-K1-ADRB1 or CHO-K1-B2 PathHunter cell lines (DiscoveRx). In this cell line, enzyme acceptor is fused to β-arrestin and enzyme donor is fused to the ADRB. Thus, activation of the ADRB1 or ADRB2 stimulates binding of β-arrestin to the ProLink-tagged ADRB1 or ADRB2 and forces complementation of the two enzyme fragments, resulting in the formation of an active β-galactosidase enzyme. Briefly, CHO-K1-ADRB1 or CHO-K1-B2 PathHunter cell lines were plated in a total volume of 20 μL cell plating reagent (DiscoveRx, 93-0563R0A) at a density of 2,500 cells/well into 384 well microplates and incubated overnight at 37°C in 5 % CO_2. The following day, 5 μL of 5X xamoterol (S-enantiomer) or 5X isoproterenol was added to cells and incubated at 37°C for 90 min. After the 90 min incubation, 15 μL of PathHunter Detection reagent cocktail (DiscoveRx, 93-0001) was added, followed by a 1 h incubation at room temperature. Chemiluminescent signal was then read with a PerkinElmer Envision™ (Perkin Elmer, MA) instrument. The results were expressed as a percent of the maximum efficacy achieved with isoproterenol.

2.2. In vitro primary microglia TNF-α assay

Mixed glial cells were obtained from the cerebral cortex of Sprague Dawley rat pups at postnatal days 1–3 and cultured in DMEM supplemented with 10% fetal bovine serum and 1% Penicillin/Streptomycin. After 10 days *in vitro*, microglia were harvested by gentle shaking of the growth flask, plated in a 96 well plate at a density of 30,000 cells/well, and incubated at 37°C overnight. Microglia were pretreated with the ADRB1 antagonists CGP 20712A (0.1 μM; Tocris 1024) or betaxolol (10 μM; Tocris 0906), the ADRB2 antagonist ICI-118551 (0.1 μM; Tocris 0821), or vehicle for 15 min. Following the pretreatment, microglia were stimulated with LPS (10 ng/ml; Sigma Aldrich L4391) along with or without xamoterol (S-enantiomer; 1 μM) or isoproterenol (1 μM; Sigma Aldrich I5627) for 4 h at 37°C. Following the 4 h incubation, cell media was collected and concentration of TNF-α was measured by ELISA (Invitrogen, KRC3011) according to the manufacturer's instruction.

2.3 5XFAD mice for in vivo studies

5XFAD mice are an aggressive model of AD-related pathology with intracellular amyloid beta and amyloid beta plaques appearing as early as 2 months (Oakley et al. 2006). 5XFAD transgenic mice overexpress 5 gene mutations related to Familial Alzheimer's Disease (FAD), 3 mutations in human AβPP (Swedish, K670N, M671L; Florida, I716V; and London, V717I) and 2 mutations in human presenilin 1 (M146L and L286V). Two independent cohorts of 40 male mice (20 5XFAD and 20 age-matched littermate controls) were used in the experiments described here (Jackson Laboratories 006554, MMRRC stock 034840; 5XFAD-Tg6799, B6SJL-Tg (APPSwFlLon, PSEN1*M146L*L286V)6799Vas/Mmjax). Mice were single-housed at the start of each experiment at 3 months of age under a reverse light-dark cycle with lights off at 8:30 AM and on at 8:30 PM. Mice were handled weekly for weight monitoring and daily prior to behavioral experiments. Individual genotypes were confirmed by PCR at the end of the experiment. All procedures related to animal maintenance and experimentation were approved by the Stanford University Administrative Panel for Laboratory Animal Care and conformed to the U.S. National Institutes of Health Guide for the Care and Use of Laboratory Animals. Efforts were made to minimize the number of mice used and their suffering. Reference to ages of mice are provided in months, rounded to the nearest 0.5 months.

2.4. *In vivo* Drug Administration

Pre-drug administration Open Field data and body weights (3 months of age) were used as pseudorandomization parameters for assigning mice to treatment groups. Following the experimental design indicated in Fig. 1, in 2x2 factor designs, wildtype and 5XFAD mice were chronically administered a selective partial agonist at the ADRB1 receptor, xamoterol (racemic mixture; Santai Pharmaceuticals) or saline vehicle. In Experiment 1, mice were administered xamoterol (6 mg/kg, oral gavage) or vehicle, 5 times per week from 4.0 to 6.5 months of age. Xamoterol was administered in the late afternoon, and, on days in which behavioral testing occurred, after testing to minimize acute effects of the drug on behavior. In order to assess effects of xamoterol at a later stage of disease progression, in Experiment 2, mice were administered xamoterol (3 mg/kg/day) or vehicle by use of a mini-osmotic pump from 7.0 to 9.5 months of age. Pumps (model 2006, Alzet, Cupertino, CA) were inserted subcutaneously in the back of each mouse under anesthesia and replaced after 6 weeks. In the older cohort (Experiment 2), as stress has been shown to accelerate markers of AD (Devi et al. 2010; Ross et al. 2015), pump administration was used as an alternative to daily dosing. Accordingly, the dose was decreased for pump administration to account for higher bioavailability via subcutaneous route, and chronic exposure. Drug doses were selected based on our previous demonstration that xamoterol crosses the blood-brain barrier and engages central nervous system targets (CREB phosphorylation) following peripheral administration in this range (Coutellier et al. 2014; Faizi et al. 2011). At time of sacrifice, plasma and brains of a subset of mice were analyzed for drug concentrations. While this design allowed us to assess efficacy of xamoterol at an early versus a late state of disease progression, due to important differences in route of administration between Experiment 1 and Experiment 2, the two cohorts were analyzed independently.

2.5. Behavioral Testing

All mice were pre-tested prior to drug administration in Open Field and Y-Maze at 3 months of age. Behavioral testing post-drug administration began 4–6 weeks after the start of drug administration (Fig. 1) and behavioral tests were performed in the order and with the timing indicated in Fig. 1. All behavioral tests were run during the dark phase of a 12-h reverse light-dark cycle. Post-drug administration tests were as follows: 6 month – oral gavage study (Social Discrimination, Open Field, Y-Maze, Novel Object Recognition (NOR), Morris Water Maze (MWM), and Fear Conditioning); 9 month – pump study (Activity Chamber, Y-Maze, NOR, MWM, Elevated Plus Maze and Fear Conditioning).

2.5.1. Open Field—General locomotor activity was assessed in a square arena (76cm x 76cm x 50cm) under low light conditions. Mice were placed in one corner of the arena and allowed to freely explore for 10 min while being tracked by an automated tracking system (Ethovision) from a ceiling-mounted camera. At the end of each trial the surface of the arena was cleaned with 1% Virkon disinfectant.

2.5.2. Activity Chamber—General locomotor activity was assessed as described previously (Faizi et al. 2011). Briefly, mice were placed in one corner of a square arena (43x 43 cm^2; MedAssociates, St. Albans Vermont) located inside of a dark sound-attenuated chamber (66×56×56 cm^3) and allowed to freely explore the arena. Movement was tracked by an automated tracking system with three planes of infrared detectors during a 10-min trial. Between each trial, the surface of the arena was cleaned with 1% Virkon disinfectant.

2.5.3. Y-maze—Y-maze was performed to assess exploration and spatial memory. The symmetrical Y-maze was made of acrylic and consisted of three arms separated by 120° angles. Each arm was 40 cm long and 8 cm wide with 15 cm high walls. Briefly, mice were placed in the center of the Y-maze and allowed to explore freely through the maze for 5 min. Arm entry was defined as having all four limbs inside an arm. The sequence and total number of arms entered were recorded. Between each trial, the surface of the arena was cleaned with 1% Virkon. A triad was defined as a set of 3 consecutive arm entries. An alternation was defined as a triad consisting of 3 unique arm entries (ex: ABC versus ABA). Percent alternation was calculated as the number of alternations divided by the total possible alternations (total entries − 2).

2.5.4. Social Discrimination—Recognition of a novel versus familiar juvenile conspecific was tested in a “homecage” social discrimination task based on (Macbeth et al. 2009). The test occurred in a clean cage and consisted of three sessions without inter-trial intervals (ITIs), one habituation session of 20-min followed by two 10-min social sessions. During the first social session (learning), an unfamiliar juvenile (4–5 weeks old) male mouse (C57BL/6J) was placed under a stainless steel wire grid cup on one side of the cage while an empty similar cup was placed on the opposite side. The position of the stimulus mouse was altered between left and right between subjects. During the second social session (recognition), the now-familiar juvenile was placed under a cup in the side of the cage that was previously containing the empty cup and a new unfamiliar C57BL/6J juvenile (not a cage-mate of the familiar juvenile) was placed under a new cup in the opposite side of the

cage. During each session, the testing animal was allowed to move freely in the entire arena for 10-min and the time spent sniffing each juvenile through the cup was recorded. The arena and cups were cleaned with 1% Virkon between mice. A discrimination index was calculated (time with novel - time with familiar) / (time with novel + time with familiar).

2.5.5. Novel Object Recognition—Mice were tested in a 20×40 cm arena to which they were habituated for 15-min the day prior to testing. On the first day of testing, mice were placed in the arena with 2 identical unfamiliar objects positioned 5 cm away from the walls. Mice were allowed to explore the arena and the objects during a 10-min trial (training session). Twenty-four hours later, one of the objects was changed for a new unfamiliar one while the other object was identical to the ones used during the training session. Again, mice were allowed to explore the arena and the objects during a 10-min trial (testing session). Each trial was recorded using an overhead camera. The amount of time spent sniffing and with the head within 1 cm of each object was scored as exploration of the object. At the end of each trial, the arena and the objects were cleaned using 1% Virkon. A discrimination index was calculated (time with novel - time with familiar) / (time with novel + time with familiar).

2.5.6. Elevated Plus Maze—Anxiety-related behavior was assessed in an elevated plus maze. Without prior habituation, mice were placed in the center intersection of an elevated (50 cm) maze with 2 opposing “open” arms (lacking walls) and 2 opposing “closed” arms (with transparent plexiglas walls). Arms were 5 cm wide by 30 cm long, and walls of closed arms were 15 cm high. Mice were allowed to explore the maze for 8 min during which behavior was recorded from a ceiling-mounted camera and analyzed with Ethovision software. Duration in and entries into open and closed arms were analyzed for both the first 5 min and the full 8 min.

2.5.7. Morris Water Maze—A modified version of the MWM was used for mice as previously reported (Nguyen et al. 2014). Mice were tested in a large water tank (178 cm in diameter; 22.0 ± 1.5°C) with a submerged 17 cm diameter circular platform (~1 cm below the water surface and ~50 cm away from the wall). Non-toxic tempera paints (Elmers) were used to make the water opaque. Privacy blinds with four different visual cues surrounded the tank and were located ~150 cm from the center of the tank. Testing was performed under dim white light (40 Lux at the water surface). Activity was monitored with Ethovision via an overhead video system. Mice completed 4–6 days of hidden platform training (60 s to locate the platform when released from a pseudorandomized drop location). Each day consisted of 4 trials (30 min intertrial intervals), and each trial ended when the mice rested on the platform for 10 s or when the trial duration expired. If trial duration expired, mice were guided to the platform. After completion of 4–6 days of hidden platform training, at 24 h after the last training session, a 60 s probe trial was conducted in the absence of the platform. Successful learning of MWM was determined by reduced escape latency during training and discriminative quadrant exploration during the probe trial. After the probe trial, the platform was moved to a new location and mice were given up to 3 days of reversal training (Reversal Training data not shown). Following reversal training, visible platform training was performed to ensure that no gross sensorimotor or visual deficits were present.

During the visible platform training, the platform was marked with a black-and-white Ping-Pong ball attached to a 10 cm wooden stick. Exclusions: 4 mice (3 wildtype-vehicle, 1 wildtype-xamoterol) from the 6 month - pump study and 1 mouse from the 9 month – pump study (wildtype-vehicle) were excluded based on lack of performance in the visual platform in conjunction with failure to demonstrate learning during hidden platform training.

2.5.8. Fear Conditioning—Conditioned fear-based learning and memory were assessed based on a previously described protocol (Faizi et al. 2012) with modifications. Conditioning and testing were performed using Coulbourn Instruments fear conditioning chambers (Whitehall, PA). A trace fear conditioning protocol was used for the training day followed by tone-cued and contextual memory retrieval tests. On the first day (conditioning), mice were placed in the chamber for a 3-min baseline recording followed by 5 tone-shock pairings with intertrial intervals (ITIs) of 100 s. The shocks (0.5 mA, 2 s) were delivered 18 s following the end of a tone (70 dB, 2 kHz, 20 s). The 18 s period following the tone and preceding the shock was defined as the TRACE period for analysis of freezing in expectation of the shock. Increased freezing in consecutive TRACE periods was used as an indication of learning. On the second day (cued recall), a novel context was used for tone-cued testing (new olfactory environment, different shape of the chamber, new texture of the floor, blue plastic inserts for walls, extra source of blue light, and visual cues). After 3 min of baseline recording, three tones without shocks with ITIs of 100 s were presented to the mice. Freezing during a TRACE period of 20 s following the tone was used as indication of cued recall. On the third day of the experiment (contextual recall), mice were placed in the same context as the first day for 5 min with no shocks or tones to test contextual memory retrieval, modified from the method described by (Saxe et al. 2006). The chambers were cleaned with simple green on days 1 and 3. On day 2, chambers were first cleaned by 1% Virkon and then wiped with wet paper towels. Freezing was defined as the complete lack of motion for a minimum of 0.75 s, as assessed by FreezeFrame software (Actimetrics, Evanston, IL). Exclusions: 3 mice were excluded from fear conditioning data in the 9 month – pump study due to lack of freezing during acquisition (less than 5% freezing: 1 wildtype-vehicle, 1 wildtype-xamoterol, 1 5XFAD-vehicle).

2.6. Cardiovascular assessment

To evaluate effects of chronic activation of ADRB1 with xamoterol on cardiac function, echocardiography was performed on 3 vehicle-treated and 3 xamoterol-treated wildtype mice from the 9 month – pump study after behavioral testing and prior to sacrifice, to measure ejection fraction, fractional shortening and heart rate. Carotid cannulation was then performed under anesthesia to measure blood pressure. After mice were sacrificed, heart weight : body weight ratio was measured and heart was fixed in 10% formalin. Hearts were serially sectioned (apex to base), and stained with Masson trichrome. Fibrosis areas within sections were measured by visualizing blue-stained areas, exclusive of staining that colocalized with perivascular or intramural vascular structures, the endocardium, or LV trabeculae. Using ImageJ, blue-stained areas and non-stained areas of each section were selected using color-based thresholding. The percentage of total fibrosis area was calculated as blue-stained areas divided by total area. The prepared slides were examined histopathologically by a board certified veterinary pathologist.

2.7. Tissue collection

Mice were deeply anesthetized with isoflurane. Prior to perfusion, whole blood was collected from the right ventricle via cardiac puncture into lithium heparin-containing vials (BD microtainer plasma tubes, Becton Dickinson 365958) for plasma collection. The right atrium was opened and mice were transcardially perfused with ice cold phosphate buffered saline (PBS, pH 7.4). Fresh brains from half of the subjects were collected, flash-frozen on liquid nitrogen and stored at −80°C for later analysis of protein and gene expression, while brains from the other half of the subjects were perfused with 4% paraformaldehyde (in PBS) and post-fixed for 24 h in the same fixative at 4 °C. Fixed brains were cryoprotected for at least 72 h (until sunk) in 30% sucrose in PBS. Fixed brains were then rapidly frozen in isopentane on dry ice. All frozen brains and plasma were stored at −80°C.

2.8. Quantitative RT-PCR

Total RNA was isolated from 50 mg of cortex using the RNeasy Lipid Tissue Mini Kit (Qiagen). One microgram of total RNA was transcribed into cDNA (Superscript III, Invitrogen). PCR was performed in duplicate using TaqMan gene expression mastermix (Applied Biosystems) and validated TaqMan gene expression assays, Iba1 (Mm00479862_g1), CD14 (Mm00438094_g1), CD74 (Mm00658576_m1), CD68 (Mm03047340_m1), IL1β (Mm00434228_m1), IL6 (Mm00446190_m1), TNF-α (Mm00443258_m1), TGFβ (Mm01178820_m1) and glyceraldehyde-3-phosphate dehydrogenase (GAPDH; Mm99999915_g1). Amplification was performed using a StepOnePlus system (Applied Biosystems). Fold changes of expression relative to control were determined after normalization to GAPDH. Relative quantification and fold change were calculated by the comparative CT method (Schmittgen and Livak 2008).

2.9. Immunohistochemistry

Immunohistochemistry was performed only in the 9 month – pump cohort and was done for a marker of microglia/macrophages, ionized calcium-binding adapter molecule-1 (Iba1), a marker of astrocytes, glial fibrillary associated protein (GFAP), amyloid beta (6E10), phosphorylated tau (AT8), and the nucleic acid stain, 4′,6-diamidino-2-phenylindole dihydrochloride (DAPI). Fixed brains were serially sectioned (at −18°C using a Microm HM-550 cryostat) in a coronal plane across 6 series through the rostrocaudal extent of the brain (40 micrometer sections; 240 micrometers between sections within each series) and stored in cryoprotectant storage buffer (30% ethylene glycol, 20% glycerol in 0.05M phosphate buffer, pH 7.4). Multilabel fluorescent immunohistochemistry was used to stain one series of brain sections for Iba1/6E10 double-label through the rostral hippocampus (from 0.26 to −2.92 mm Bregma) and one series for GFAP/6E10 double-label through rostral piriform and cingulate cortices (1.98 to 0.50 mm Bregma) (Paxinos and Franklin 2001). Phosphorylated tau was visualized with single-label avidin-biotin-peroxidase (SG Chromagen) immunohistochemistry (AT8 antibody) in one series of brain sections through the forebrain (0.00 to 0.26 mm Bregma).

Multilabel Fluorescent IHC—Free-floating sections were incubated at room temperature in 24-well tissue culture plates gently shaken on an orbital shaker throughout the procedure.

All rinses were 15 min unless stated otherwise. Sections were rinsed three times in 0.05 M PBS, and then preincubated 1 h in PBS containing 1% Triton X-100 (PBST) and 6% normal donkey serum. Sections were incubated 18 h with rabbit anti-Iba1 primary antibody (019-19741, Wako Chemicals USA, Richmond, VA, USA) diluted 1:1000 or chicken anti-GFAP (ab4674, Abcam, Cambridge, MA, USA) diluted 1:1000 and mouse anti-6E10 primary antibody (803001, Biolegend, San Diego, CA, USA; binds to amino acid residue 1–16 of amyloid beta) diluted 1:1000 in 0.3% PBST and 2% normal donkey serum. Following 3 PBS rinses, sections were incubated for 2 h in CY3-conjugated donkey anti-rabbit (711-165-152, Jackson Immunoresearch, Bar Harbor, ME) or 594-conjugated donkey anti-chicken (703-585-155, Jackson Immunoresearch) and AlexaFluor 488-conjugated donkey anti-mouse (715-545-151, Jackson Immunoresearch) IgG secondary antibodies each diluted 1:200 in PBS. Sections were then rinsed 2 times prior to incubation for 30 min with DAPI (D9542, Sigma-Aldrich, St. Louis, MO) diluted 1:5000 in PBS. Free-floating sections were then rinsed 3 times in PBS, rinsed briefly in 0.15% gelatin in water, mounted on clean glass slides, and allowed to air-dry to affix sections to slides immediately prior to coverslipping with polyvinyl alcohol mounting medium with DABCO antifade (10981, Sigma-Aldrich).

Avidin-biotin-peroxidase IHC (AT8-immunoreactivity)—Protocol was the same as above with the following exceptions. Prior to the initial blocking step, sections were incubated in 1% hydrogen peroxide in PBS for 15 min followed by 2x15 min washes. Following the overnight primary incubation, sections were incubated in biotinylated goat anti-mouse secondary antibody (1:400 concentration, 90 min; Sigma SAB3701075) followed by 2x15 min washes and an incubation with an avidin-biotin complex solution (Vector ABC, 1:200, 60 min). SG chromagen (Vector SK4705) was used to visualize the antibody complex. Slides were coverslipped with Cytoseal XYL (Richard-Allen Scientific, 8312-4).

Image analysis—Regions of analysis were selected in the hippocampal complex, amygdala, and cortex based on anatomical evidence for terminal projections from LC and involvement in learning and memory (Corcoran et al. 2016; Todd and Bucci 2015; Samuels and Szabadi 2008; Murchison et al. 2004). Iba1-immunoreactivity (*-ir*) and 6E10-*ir* were assessed in retrosplenial cortex (RS), lateral/basolateral amygdala (LA/BLA), CA3 region of the hippocampus, dentate gyrus (DG), and subiculum (SUB) across 3–6 consecutive serial sections (depending on structure) throughout the respective structures (see Fig. 2 for depiction of regions of interest). GFAP-*ir* and 6E10-*ir* were assessed in piriform (Pir) and cingulate cortices (Cg) across 6–8 rostrocaudal levels throughout the extent of the structures (see Fig. 3). Due to limited tissue availability, AT8-*ir* was quantified only in RS, as a representative region with substantial amyloid beta and tau pathology in the 5XFAD model. Immunostaining was quantified in both left and right hemispheres at multiple rostrocaudal levels without differentiation of hemisphere for analysis. Images were captured under consistent exposure settings at 5X or 10X magnification using a Zeiss Axioscope M2 microscope with Stereo Investigator 10.0 Software (MicroBrightField Bioscience, VT). Images were quantified using NIH ImageJ 1.49. Fluorescence RGB images were converted to RGB monochrome stacks for image quantification. Regions were first outlined in the DAPI monochrome stack, “mean gray value” was quantified within the Iba1 or GFAP

stacks, and % area was quantified within the 6E10 stack which was thresholded based on 6E10-*ir*. AT8-*ir* was converted to a monochrome image and % area was quantified using a thresholding function. Each image was quantified 3 times and an average value (accounting for intra-evaluator variation) was obtained for each image. Average values for each structure were analyzed in GraphPad Prism 5.0 software.

2.10. Calculation and Statistics

In vitro pharmacology data were calculated from a number of independent experiments performed in replicates as indicated. Curve fitting was performed with Prism 5.0 (GraphPad Software) using the equation for a single-site sigmoidal, dose-response curve with a variable slope. EC_{50} values are expressed as geometric means (95% confidence limits). Statistical analyses were performed with IBM SPSS Statistical Package 22.0 and Prism 5.0. Repeated measures, one-way or two-way analyses of variance were followed by post-hoc comparison of select treatment groups with Bonferroni's or Dunnett's tests correcting for multiple comparisons. Significance was accepted at $p < .05$.

3. Results

3.1. Xamoterol is a selective ADRB1 partial agonist with functional bias for the cAMP signaling pathway

Xamoterol showed partial agonist activity on the cAMP pathway (50.0 ± 5.0 % relative to the full agonist, isoproterenol) through the ADRB1 receptor with an EC_{50} of 2.2 nM (0.3 – 14.6 nM) and no cAMP activity through either ADRB2 or ADRB3 up to 100 μM (See Fig. 2A). Xamoterol had minimal (<10%) activation of the β-arrestin pathway through ADRB1 and none through ADRB2 at concentrations up to 30 μM (Fig. 2B).

3.2. Xamoterol attenuated LPS-induced TNF-α production in primary rat microglia culture through ADRB1

Both the ADRB1-selective partial agonist, xamoterol (1 μM), and the non-selective full agonist, isoproterenol (1 μM), had anti-inflammatory properties *in vitro* as measured by a reduction in LPS-induced TNF-α production in primary rat microglia (Fig. 3). Anti-inflammatory effects of xamoterol were less than that of isoproterenol and were reversed with ADRB1-selective antagonists, CGP 20712A (0.1 μM) or betaxolol (10 μM) but not the ADRB2 antagonist ICI-118551 (0.1 μM). Anti-inflammatory effects of isoproterenol were partially reversed by both betaxolol and ICI-118551 although CGP 20712A had no effect.

3.3. Xamoterol was detectable in the brain following chronic dosing in mice

Three mice were randomly selected from each of the two independent *in vivo* chronic dosing experiments for analysis of brain concentrations of xamoterol at time of sacrifice. Xamoterol concentrations were detected at 2.14 ± 0.42 ng/g for Experiment 1 (wildtype; n=3; approximately 18–24 h after last oral gavage administration) and 4.27 ± 1.6 ng/g for Experiment 2 (wildtype; n=3; pump administration). For comparison, mean terminal plasma concentrations of xamoterol from the same subjects following pump administration in Experiment 2 were 12.46 ± 1.83 ng/mL (n=3). Terminal plasma was not measured for gavage administration as xamoterol is known to be cleared within 6–8 hours from the

periphery and would not be have been expected to be detectable at 18–24 hours after dosing. Comparison of means revealed no significant difference in brain concentrations between dosing routes at the terminal timepoint (t-test; t(4) = 1.254; p = .278).

3.4. Chronic administration of the ADRB1 partial agonist, xamoterol, had no effect on bodyweight or cardiovascular function in 5XFAD mice

No effects of genotype or chronic administration of xamoterol were observed on bodyweight in the 6 month-oral gavage study (data not shown). 5XFAD mice had lower bodyweight than wildtype mice in the 9 month-pump study (two-way analysis of variance, $F_{(1,33)} = 4.311$; p = .046; data not shown). There were no effects of chronic administration of xamoterol on bodyweight.

As ADRB1 receptors are expressed in cardiovascular tissue, we examined the effects of chronic low dose administration of the ADRB1 partial agonist, xamoterol, on cardiovascular function in a sample of wildtype mice from the 9 month-pump study. No effects on cardiovascular function or structure (blood pressure, heart rate, echocardiography or fibrosis) were observed with this chronic low dose administration (Fig. S1).

3.5. Peripheral administration of the ADRB1 partial agonist, xamoterol, attenuated inflammation-related mRNA expression in 5XFAD mice

Cortical dissections from fresh-frozen brains from Experiments 1 and 2 were assessed for mRNA expression for genes related to neuroimmune activation (See Table 1 for list of genes; Fig. 4 for results; Table S1 for ANOVA).

Six month – oral gavage study—All genes (Iba1, TNF-α, IL1β, IL-6, CD14, TGFβ, and CD68), with the exception of CD74, were elevated in 5XFAD-vehicle treated mice relative to wildtype-vehicle in the 6 month-oral gavage study (Fig. 4A–H; Table S1). Higher mean mRNA expression of CD74 in 5XFAD-vehicle mice was not significant. Trends for attenuation of elevated expression of TNF-α and CD14 with xamoterol were observed, but did not reach significance.

Nine month – pump study—All genes (Iba1, TNFα, IL1β, CD14, CD74, TGFβ CD68) with the exception of IL6, were elevated in 5XFAD-vehicle treated mice relative to wildtype-vehicle (Fig. 4I–P; Table S1). Chronic treatment with xamoterol attenuated elevated expression of Iba1, CD74, CD14 and TGFβ. Notably, elevated expression of CD68, a marker of phagocytosis, in 5XFAD mice was further elevated with xamoterol treatment in both cohorts, although this potentiation did not reach significance in either study (Fig. 4H,P).

3.6. Chronic peripheral administration of the ADRB1 partial agonist, xamoterol, reduced immunohistochemical indices of microgliosis, astrogliosis, amyloid beta pathology and tau pathology

5XFAD transgenic mice present an aggressive model for amyloid beta deposition which occurs between 1.5 and 2 months (Oakley et al. 2006). Immunohistochemical analyses of amyloid beta (6E10)-*ir* alongside microglia/macrophage (Iba1)-*ir* and astrocyte (GFAP)-*ir*,

as well as evidence for phosphorylated tau (AT8)-*ir* were assessed in tissue from the 9 month – pump study. Low sample size due to perfusion artifact prevented IHC analysis from the 6 month – oral gavage study.

Double-label immunohistochemistry revealed Iba1-*ir* and GFAP-*ir* cells in close proximity to amyloid beta deposits (6E10-*ir*), as has been reported (Kalinin et al. 2007; Dhawan et al. 2012; Kan et al. 2015; Savage et al. 2015; Girard et al. 2014) (Figs. 5 and 6). Elevated Iba1-*ir* and GFAP-*ir* were detected in 5XFAD vehicle-treated mice relative to wildtype mice in all regions analyzed and these increases in both Iba1-*ir* and GFAP-*ir* were attenuated in all regions with chronic administration of the selective ADRB1 partial agonist, xamoterol (Figs. 5C and 6C).

Quantification of AT8 immunostaining in retrosplenial cortex revealed elevations in AT8-*ir* in 5XFAD-vehicle versus wildtype-vehicle mice (Fig. 7). These elevations were attenuated in xamoterol-treated 5XFAD mice.

Chronic treatment with the selective ADRB1 partial agonist, xamoterol, reduced 6E10-*ir* in 5XFAD mice in DG and CA3 and resulted in tendencies for a decrease in 6E10-*ir* in RS ($t(6) = 1.973$; $p = .096$), Cg ($t(8) = 1.938$; $p = .089$) and Pir/En ($t(8) = 1.648$; $p = .138$) that did not reach significance (Figs. 5B and 6B). Xamoterol administration did not alter 6E10-*ir* in LA/BLA, or SUB.

3.7 No deficits in cognitive function were observed in 5XFAD mice

Cognitive function was assessed over a 5–6 week period starting at least 6 weeks into the chronic drug administration for each experiment (refer to Fig. 1 for timing of drug administration relative to behavioral testing). No behavioral deficits were observed for vehicle-treated 5XFAD mice relative to wildtype counterparts in any behavioral test in either study (Tables 2 and 3) and therefore there were no grounds for assessing treatment efficacy on behavior. A notable trend for a deficit in NOR in the 6 month – oral gavage cohort was observed for the 5XFAD vehicle-treated group but not their xamoterol-treated counterparts. This same pattern was recapitulated in the NOR task in the 9 month - pump study, but again did not reach significance. All groups showed evidence for learning in the MWM based on a decrease in escape latency across days, and no deficits in acquisition were observed in 5XFAD relative to wildtype mice. Fear Conditioning was not assessed in Experiment 1 as group means for freezing during the acquisition phase did not exceed 20%, including in vehicle-treated wildtype control mice. In the 9 month – pump study, no group differences were observed for freezing behavior during acquisition, cued recall, or contextual recall of freezing behavior (Table 3).

4. Discussion

AD is characterized by amyloid beta plaque deposition and tau pathology associated with neuronal degeneration, neuroinflammation and cognitive dysfunction. 5XFAD transgenic mice are a robust model for amyloid beta deposition, and indeed here we observe evidence for both amyloid beta pathology and phosphorylated tau pathology. We report robust evidence for neuroinflammation in 5XFAD transgenic mice (e.g. microglia/macrophage and

astrocyte markers and neuroimmune-related gene expression). In order to investigate the role of beta-adrenergic systems in modulation neuroinflammation and pathology, we first provided evidence that the beta adrenergic partial agonist, xamoterol, is not only highly selective for ADRB1 and functionally biased for the cAMP pathway at the human receptor *in vitro*, but also has ADRB1-selective anti-inflammatory effects in a primary rat microglia culture. Then, in the 5XFAD mouse model, chronic administration of xamoterol attenuated indices of neuroinflammation and reduced both amyloid beta and tau pathology. We did not observe robust behavioral deficits in the 5XFAD mouse model and discuss possible explanations for this below. Reductions in bodyweight in 5XFAD relative to wildtype mice in the 9 month cohort, but not in the younger cohort are in line with previous reports (Jawhar et al. 2012). Additionally, despite presence of ADRB1 in cardiovascular tissue, no alteration of cardiac function was observed following chronic low dose activation of ADRB1 with xamoterol. While ADRB1 has previously been shown to be important for learning and memory (Murchison et al. 2004), data reported here suggest for the first time that chronic partial agonism of the ADRB1 receptor may attenuate neuroinflammation and pathology at both early and late stage disease progression, with potential for therapeutic benefit in AD.

Xamoterol is a highly selective partial ADRB1 agonist with functional bias for cAMP over the β-arrestin pathway

Xamoterol has previously been shown to bind to ADRB1 with high affinity (K_D of 60.25), exhibiting 14-fold selectivity over ADRB2 (K_D of 851nM) and more than 500-fold selectivity over ADRB3 (K_D of 35,481 nM). (Baker 2005). Our data show that in a functional assay using human beta adrenergic receptors and measuring cAMP response, xamoterol activated ADRB1 with an EC_{50} of 2 nM and an efficacy of ~ 50% of the cAMP pathway response relative to the full agonist isoproterenol. On the other hand, xamoterol did not activate the cAMP pathway via the ADRB2 or ADRB3 receptors (up to 100 uM). Collectively, these data suggest that xamoterol is highly selective and can be a useful pharmacological tool to study pathways related to ADRB1. Another important pharmacological property of xamoterol discovered in this study is its functional selectivity for the cAMP pathway against the β-arrestin pathway. In a classic view of G-protein coupled receptors, ADRB1 agonist would activate adenylyl cyclase and increase cAMP levels. At the same time, ADRB1 activation would stimulate recruitment of β-arrestin to the receptor, leading to receptor desensitization (Pierce and Lefkowitz 2001; Freedman and Lefkowitz 1996; Zhang et al. 1997). However, it has become clear that agonists can show biased activation of signaling pathways in an agonist-specific manner (Rajagopal et al. 2010; Allen et al. 2011; Violin and Lefkowitz 2007; Maillet et al. 2015). In the case of xamoterol, it selectively activated the cAMP pathway while maintaining minimal (~10%) activity on the β-arrestin pathway. To our knowledge, this is the first report of a cAMP pathway biased agonist of ADRB1. As β-arrestin signaling mediates multiple cellular functions including receptor desensitization and agonist-induced tolerance (Freedman and Lefkowitz 1996; Zhang et al. 1997), functional bias against the β-arrestin mediated signaling activity may have important clinical implications in CNS disorders and require further investigation.

Xamoterol attenuates amyloid beta and tau pathology in 5XFAD mice

Chronic xamoterol treatment reduced amyloid beta, as measured by regional immunohistochemistry in regions of the hippocampal complex. This reduction in amyloid beta is in accordance with previous studies demonstrating that broadly increasing adrenergic tone with the NA precursor, L-DOPS, in transgenic mice overexpressing human AβPP, decreases plaque load, (Kalinin et al. 2012; Heneka et al. 2010). These effects have been attributed to mechanisms such as enhanced microglia phagocytosis of amyloid beta, or increased activity of amyloid beta degrading enzymes such as neprilysin. NA has been shown to directly stimulate phagocytosis of amyloid beta in mouse microglia cultures *in vitro* (Heneka et al. 2010; Kalinin et al. 2007) although the receptor subtype specificity of this effect has not been clearly demonstrated. We did not examine potential effects on phagocytosis or amyloid beta processing in the current study and future studies will address these questions from the context of adrenergic receptor subtype specificity. Whether through modulating AβPP processing, degradation of amyloid beta, or microglial phagocytosis of amyloid beta, noradrenergic tone has been shown to modulate amyloid beta plaque load, and our data suggest that ADRB1 may contribute to these effects.

In addition to amyloid beta pathology, we report immunohistochemical evidence for phosphorylated tau pathology in cortex of 5XFAD mice that is attenuated with chronic xamoterol treatment. Presence of tau pathology in this 5XFAD model is supported by previous work suggesting that tau pathology may be downstream from amyloid beta pathology (Blanchard et al. 2003; Saul et al. 2013). It therefore remains a possibility that attenuation of tau pathology with xamoterol is downstream from effects of xamoterol on amyloid beta pathology.

Xamoterol modulates neuroinflammation

While adrenergic systems have been known to modulate the peripheral immune system, our data support recently accumulating evidence for similar neuroimmunomodulatory roles for noradrenergic tone in the brain. NA has been shown to directly suppress cytokine and chemokine responses to amyloid beta in microglia cultures *in vitro* including suppression of MHCII, TNF-α, IL1β and iNOS signaling (Heneka et al. 2010). Additionally, deficits in NA exacerbate inflammatory responses to amyloid beta *in vivo* (Heneka et al. 2002). Here we demonstrate attenuation of an inflammatory profile in both an acute primary rat microglia culture model of inflammation and in a chronic 5XFAD mouse model of AD with a highly selective and functionally biased ADRB1 partial agonist.

Given parallel reductions in indices of inflammation and amyloid beta and tau pathology in the present study, it is difficult to determine whether attenuation of pro-inflammatory markers is due to direct anti-inflammatory actions of xamoterol, or is secondary to reductions in pathology. A direct anti-inflammatory action is supported by *in vitro* evidence presented here that xamoterol (via ADRB1) and isoproterenol (via ADRB1 and ADRB2) can suppress TNF-α production in rat primary microglia challenged with LPS. This supports previous work showing that primary microglia cells express both ADRB1 and ADRB2 and NA and compounds with moderate selectivity for ADRB1 or ADRB2, dobutamine and terbutaline, directly suppress pro-inflammatory cytokines in these primary cultures (Mori et

al. 2002). A secondary action is supported by trends observed in the current study for an increase in CD68 expression in both cohorts of 5XFAD mice treated with xamoterol. CD68 is involved in phagocytosis (Fu et al. 2014) and this potentiation could indicate an ADRB1-mediated increase in phagocytosis, which could contribute to observed reductions in amyloid beta and consequent reduction in pro-inflammatory markers. This is supported by previous *in vivo* and *in vitro* evidence that adrenergic receptors can stimulate microglial phagocytosis of amyloid beta (Heneka et al. 2010), and here we provide the first set of experimental data suggesting that ADRB1 may contribute to this process, a process which could be pharmacologically controlled. We also cannot exclude the possibility that effects of xamoterol in the periphery are contributing to or mediating effects on neuroinflammation in the present study. Indeed, the important role of the adaptive immune system in AD-related pathology has recently been highlighted in the 5XFAD AD model (Marsh et al. 2016) and is an area in which we are currently investigating in the context of the adrenergic system.

While we have shown that xamoterol is very selective for the human ADRB1 receptor compared to human ADRB2 and ADRB3 receptors, and while the high homology between human, mouse and rat ADRB1 (100% at the binding sites based on protein sequence alignment) and the selective pharmacological effects shown here in isolated rodent microglia preparations suggest that ADRB1 is a strong contributor to the anti-inflammatory effects we observe in the 5XFAD mouse model of AD, we cannot exclude the possibility that ADRB2 may contribute to anti-inflammatory effects in our mouse models of AD. It has been previously reported for mouse beta receptors *in vitro*, that xamoterol in high concentration can activate both ADRB1 and ADRB2, where the efficacy of xamoterol for cAMP production by ADRB2 is ~30% of that for ADRB1 (Murchison et al. 2004). In addition, Murchison et al have shown that, in *in vivo* mouse studies, xamoterol activates ADRB2 signaling in the CNS at a dose range (~0.6–6 mg/kg) that overlaps with that for ADRB1 (0.3–3 mg/kg) (Murchison et al. 2004; Schutsky et al. 2011b), and whereas cognitive enhancing effects of low doses of xamoterol are ADRB1-dependent, high doses of xamoterol impair memory retrieval in mice, effects that are reversed with a selective ADRB2 antagonist, but not a selective ADRB1 antagonist (Schutsky et al. 2011b). While we present some of the first evidence that anti-inflammatory effects of xamoterol may be ADRB1-mediated, we think that ADRB1 and ADRB2 both have anti-inflammatory actions as the anti-inflammatory effect of the non-selective full agonist, isoproterenol are only partially reversed by each of a selective ADRB1 or ADRB2 antagonist. Indeed others have reported on anti-inflammatory actions of ADRB2, and both receptors should be considered as therapeutic targets (Qian et al. 2011; Ryan et al. 2013).

Behavior in the 5XFAD model of AD

We did not observe behavioral deficits in transgenic animals in any task, including Y-Maze and Contextual Fear Conditioning, for which the most robust behavioral deficits have previously been reported for this model (Oakley et al. 2006; Kimura and Ohno 2009). Deficits in Y-maze alternation have been reported as early as 4–5 months (Oakley et al. 2006) and in Contextual Fear Conditioning as early as 6–8 months (Kaczorowski et al. 2011; Ohno 2009). In the present study, mice were tested on Y-maze at 3 months and 5 months (Experiment 1) and 3 months and 8 months (Experiment 2). It is possible that we would only

have expected to see robust deficits in the older males in Experiment 2. A shorter testing session (5 min) than in previous reports (8 min), testing during the active phase (dark cycle), as well as repeat testing in the Y-Maze and exposure to multiple behavioral paradigms (form of enrichment) are potential procedural differences that may differentiate the present studies. Regarding Contextual Fear Conditioning, it has been previously reported that the deficit commonly reported for 6 months and older 5XFAD mice is accomplished with a single CS-US pairing and is not seen when mice are trained with 3–5 shocks (Kimura and Ohno 2009), as was done in the present study (5 pairings). Additionally, contextual fear conditioning has been reported in a 24 h paradigm, whereas in the current study, we assessed *cued* recall at 24 h and contextual recall at 48 h. These differences may explain the present lack of these two most robustly reported behavioral deficits in this line. Additionally, lack of behavioral deficits in 5XFAD mice relative to wildtype mice in this study might be related to poor performance in the wildtype group due to a combination of factors such as chronic social isolation (all mice were single-housed), stress of the chronic drug administration in the 6 month - oral gavage cohort and repeated behavioral testing in both cohorts. Another consideration is that while the 5XFAD model was originally developed on a B6/SJL background, the same background as in the present study, a large number of reports of behavioral deficits in 5XFAD mice come from lines that were backcrossed with a C57BL6/J line to facilitate comparison with other lines.

We did not observe deficits in the MWM at 6 months (Experiment 1) or 9 months (Experiment 2) and others have also reported a lack of deficit in MWM at 3 and 6 months in this same line (Schneider et al. 2014). We did not observe any deficits in 5XFAD mice in the EPM at 9 months (Experiment 2) although reduced anxiety in the Elevated Plus Maze has been reported for males on the B6/SJL background (Schneider et al. 2015). Deficits in NOR have been reported at 7 months on the B6/SJL background (Modi et al. 2014), but we only observed non-significant decreases in discrimination ratio in 5XFAD mice both at 6 months (Experiment 1) and at 8 months (Experiment 2). We report no deficits in Social Discrimination behavior in the 5XFAD model at 5 months of age (Experiment 1). 5XFAD mice have been shown to have normal locomotor behavior in the Open Field (at least through 9 months) (Jawhar et al. 2012) as we report here.

Conclusions

Numerous experimental therapeutics with positive preclinical results have failed to generate positive outcomes in human AD trials. New insights and innovative approaches are essential to provide relief and ultimately prevent, delay or cure the pathological progression of AD. One novel strategy is to look to the body’s natural defense mechanisms, such as the noradrenergic system, which has been demonstrated to be compromised in AD patients. Polymorphisms in the human ADRB1 gene contribute to a genetic risk factor for development of AD (Bullido et al. 2004). Here we demonstrate that noradrenergic tone contributes to modulation of amyloid beta and tau pathology and neuroinflammation. Increasing tone specifically at the ADRB1 receptor may help to improve both underlying pathology and cognitive deficits related to AD. While epidemiological studies linking use of adrenergic beta-blockers for cardiovascular indications to AD susceptibility or rate of functional decline in AD patients might be expected to reveal a heightened susceptibility or

increased rate of functional decline, studies have yielded mixed results, including an association with *delayed* functional decline (Rosenberg et al. 2008). Factors such as BBB permeability of beta blockers, pharmacological specificity of different beta-blockers, as well as an important role for cardiovascular function and hypertension in AD disease pathology may contribute to the current lack of clarity on this issue. Further elucidation is required on mechanisms through which deficits in NA neurotransmission and consequent dysregulation of the central and/or systemic immune responses are contributing to disease progression and cognitive and neuroinflammatory symptoms of AD. We have proposed that restoration of adrenergic tone at the ADRB1 receptor could slow or prevent AD-related pathology and alleviate cognitive deficits related to AD. Of central importance is deciphering how NA and the NA receptors contribute to AD. What is the role of central NA in regulation of neuroimmune function? How are these functions affected in AD? What are the consequences of selectively restoring noradrenergic receptor subtype signaling for cognition, pathology and neuroimmune function? We are continuing to study and investigate these mechanistic questions in our laboratory.

Supplementary Material

Refer to Web version on PubMed Central for supplementary material.

Acknowledgments

This study was partially supported by NINDS 5 P30 NS069375 05. Cardiac histopathology was performed by Richard Luong at Stanford University. We thank Mingming Zhao from Daniel Bernstein's Lab at Stanford University for expert assistance with echocardiography and blood pressure recordings. We thank Nay Lui Saw for excellent technical assistance for behavioral studies.

Abbreviations

6E10	anti-amyloid beta antibody
AD	Alzheimer's disease
ADRB1, 2, 3	beta1, 2, 3 adrenergic receptors
AT8	anti-phosphorylated tau antibody
AβPP	amyloid beta protein precursor
Cg	cingulate cortex
DAPI	4′,6-diamidino-2-phenylindole dihydrochloride
DG	dentate gyrus
En	endopiriform cortex
FAD	familiar Alzheimer's disease
GAPDH	glyceraldehyde-3-phosphate dehydrogenase
GFAP	glial fibrillary associated protein

Iba1	ionized calcium-binding adapter molecule-1
-ir	immunoreactivity
ITI	inter-trial intervals
LA/BLA	lateral and basolateral amygdala
LC	locus coeruleus
LSD	Least Significant Difference
MWM	Morris water maze
NA	noradrenergic
NOR	novel object recognition
PBS	phosphate-buffered saline
PBST	PBS containing 1% Triton X-100
Pir	piriform cortex
RS	retrosplenial cortex
SUB	subiculum

Reference List

1. Allen JA, Yost JM, Setola V, Chen X, Sassano MF, Chen M, et al. Discovery of beta-arrestin-biased dopamine D2 ligands for probing signal transduction pathways essential for antipsychotic efficacy. Proc Natl Acad Sci U S A. 2011; 108:18488–18493. [PubMed: 22025698]
2. Baker JG. The selectivity of beta-adrenoceptor antagonists at the human beta1, beta2 and beta3 adrenoceptors. Br J Pharmacol. 2005; 144:317–322. [PubMed: 15655528]
3. Blanchard V, Moussaoui S, Czech C, Touchet N, Bonici B, Planche M, et al. Time sequence of maturation of dystrophic neurites associated with Abeta deposits in APP/PS1 transgenic mice. Exp Neurol. 2003; 184:247–263. [PubMed: 14637096]
4. Bondareff W, Mountjoy CQ, Roth M, Rossor MN, Iversen LL, Reynolds GP, et al. Neuronal degeneration in locus ceruleus and cortical correlates of Alzheimer disease. Alzheimer Dis Assoc Disord. 1987; 1:256–262. [PubMed: 3453748]
5. Braak H, Thal DR, Ghebremedhin E, Del TK. Stages of the pathologic process in Alzheimer disease: age categories from 1 to 100 years. J Neuropathol Exp Neurol. 2011; 70:960–969. [PubMed: 22002422]
6. Branca C, Wisely EV, Hartman LK, Caccamo A, Oddo S. Administration of a selective beta2 adrenergic receptor antagonist exacerbates neuropathology and cognitive deficits in a mouse model of Alzheimer's disease. Neurobiol Aging. 2014; 35:2726–2735. [PubMed: 25034342]
7. Bullido MJ, Ramos MC, Ruiz-Gomez A, Tutor AS, Sastre I, Frank A, et al. Polymorphism in genes involved in adrenergic signaling associated with Alzheimer's. Neurobiol Aging. 2004; 25:853–859. [PubMed: 15212839]
8. Bylund DB, Eikenberg DC, Hieble JP, Langer SZ, Lefkowitz RJ, Minneman KP, et al. International Union of Pharmacology nomenclature of adrenoceptors. Pharmacol Rev. 1994; 46:121–136. [PubMed: 7938162]

9. Corcoran KA, Frick BJ, Radulovic J, Kay LM. Analysis of coherent activity between retrosplenial cortex, hippocampus, thalamus, and anterior cingulate cortex during retrieval of recent and remote context fear memory. Neurobiol Learn Mem. 2016; 127:93–101. [PubMed: 26691782]
10. Coutellier L, Ardestani PM, Shamloo M. beta1-adrenergic receptor activation enhances memory in Alzheimer's disease model. Ann Clin Transl Neurol. 2014; 1:348–360. [PubMed: 24883337]
11. Cunningham C, Campion S, Lunnon K, Murray CL, Woods JF, Deacon RM, et al. Systemic inflammation induces acute behavioral and cognitive changes and accelerates neurodegenerative disease. Biol Psychiatry. 2009; 65:304–312. [PubMed: 18801476]
12. Day JS, O'Neill E, Cawley C, Aretz NK, Kilroy D, Gibney SM, et al. Noradrenaline acting on astrocytic beta(2)-adrenoceptors induces neurite outgrowth in primary cortical neurons. Neuropharmacology. 2014; 77:234–248. [PubMed: 24126345]
13. Devi L, Alldred MJ, Ginsberg SD, Ohno M. Sex- and brain region-specific acceleration of beta-amyloidogenesis following behavioral stress in a mouse model of Alzheimer's disease. Mol Brain. 2010; 3:34. [PubMed: 21059265]
14. Dhawan G, Floden AM, Combs CK. Amyloid-beta oligomers stimulate microglia through a tyrosine kinase dependent mechanism. Neurobiol Aging. 2012; 33:2247–2261. [PubMed: 22133278]
15. Faizi M, Bader PL, Saw N, Nguyen TV, Beraki S, Wyss-Coray T, et al. Thy1-hAPP(Lond/Swe+) mouse model of Alzheimer's disease displays broad behavioral deficits in sensorimotor, cognitive and social function. Brain Behav. 2012; 2:142–154. [PubMed: 22574282]
16. Faizi M, Bader PL, Tun C, Encarnacion A, Kleschevnikov A, Belichenko P, et al. Comprehensive behavioral phenotyping of Ts65Dn mouse model of Down syndrome: activation of beta1-adrenergic receptor by xamoterol as a potential cognitive enhancer. Neurobiol Dis. 2011; 43:397–413. [PubMed: 21527343]
17. Freedman NJ, Lefkowitz RJ. Desensitization of G protein-coupled receptors. Recent Prog Horm Res. 1996; 51:319–351. [PubMed: 8701085]
18. Fu R, Shen Q, Xu P, Luo JJ, Tang Y. Phagocytosis of microglia in the central nervous system diseases. Mol Neurobiol. 2014; 49:1422–1434. [PubMed: 24395130]
19. Fujita H, Tanaka J, Maeda N, Sakanaka M. Adrenergic agonists suppress the proliferation of microglia through beta 2-adrenergic receptor. Neurosci Lett. 1998; 242:37–40. [PubMed: 9509999]
20. German DC, Manaye KF, White CL III, Woodward DJ, McIntire DD, Smith WK, et al. Disease-specific patterns of locus coeruleus cell loss. Ann Neurol. 1992; 32:667–676. [PubMed: 1449247]
21. Girard SD, Jacquet M, Baranger K, Migliorati M, Escoffier G, Bernard A, et al. Onset of hippocampus-dependent memory impairments in 5XFAD transgenic mouse model of Alzheimer's disease. Hippocampus. 2014; 24:762–772. [PubMed: 24596271]
22. Heneka MT, Galea E, Gavriluyk V, Dumitrescu-Ozimek L, Daeschner J, O'Banion MK, et al. Noradrenergic depletion potentiates beta -amyloid-induced cortical inflammation: implications for Alzheimer's disease. J Neurosci. 2002; 22:2434–2442. [PubMed: 11923407]
23. Heneka MT, Nadrigny F, Regen T, Martinez-Hernandez A, Dumitrescu-Ozimek L, Terwel D, et al. Locus ceruleus controls Alzheimer's disease pathology by modulating microglial functions through norepinephrine. Proc Natl Acad Sci U S A. 2010; 107:6058–6063. [PubMed: 20231476]
24. Heneka MT, Ramanathan M, Jacobs AH, Dumitrescu-Ozimek L, Bilkei-Gorzo A, Debeir T, et al. Locus ceruleus degeneration promotes Alzheimer pathogenesis in amyloid precursor protein 23 transgenic mice. J Neurosci. 2006; 26:1343–1354. [PubMed: 16452658]
25. Jawhar S, Trawicka A, Jenneckens C, Bayer TA, Wirths O. Motor deficits, neuron loss, and reduced anxiety coinciding with axonal degeneration and intraneuronal Abeta aggregation in the 5XFAD mouse model of Alzheimer's disease. Neurobiol Aging. 2012; 33:196–40.
26. Kaczorowski CC, Sametsky E, Shah S, Vassar R, Disterhoft JF. Mechanisms underlying basal and learning-related intrinsic excitability in a mouse model of Alzheimer's disease. Neurobiol Aging. 2011; 32:1452–1465. [PubMed: 19833411]
27. Kalaria RN, Andorn AC, Tabaton M, Whitehouse PJ, Harik SI, Unnerstall JR. Adrenergic receptors in aging and Alzheimer's disease: increased beta 2-receptors in prefrontal cortex and hippocampus. J Neurochem. 1989; 53:1772–1781. [PubMed: 2553864]

28. Kalinin S, Gavrilyuk V, Polak PE, Vasser R, Zhao J, Heneka MT, et al. Noradrenaline deficiency in brain increases beta-amyloid plaque burden in an animal model of Alzheimer's disease. Neurobiol Aging. 2007; 28:1206–1214. [PubMed: 16837104]
29. Kalinin S, Polak PE, Lin SX, Sakharkar AJ, Pandey SC, Feinstein DL. The noradrenaline precursor L-DOPS reduces pathology in a mouse model of Alzheimer's disease. Neurobiol Aging. 2012; 33:1651–1663. [PubMed: 21705113]
30. Kan MJ, Lee JE, Wilson JG, Everhart AL, Brown CM, Hoofnagle AN, et al. Arginine deprivation and immune suppression in a mouse model of Alzheimer's disease. J Neurosci. 2015; 35:5969–5982. [PubMed: 25878270]
31. Kimura R, Ohno M. Impairments in remote memory stabilization precede hippocampal synaptic and cognitive failures in 5XFAD Alzheimer mouse model. Neurobiol Dis. 2009; 33:229–235. [PubMed: 19026746]
32. Koronyo-Hamaoui M, Ko MK, Koronyo Y, Azoulay D, Seksenyan A, Kunis G, et al. Attenuation of AD-like neuropathology by harnessing peripheral immune cells: local elevation of IL-10 and MMP-9. J Neurochem. 2009; 111:1409–1424. [PubMed: 19780903]
33. Lambert JC, Grenier-Boley B, Chouraki V, Heath S, Zelenika D, Fievet N, et al. Implication of the immune system in Alzheimer's disease: evidence from genome-wide pathway analysis. J Alzheimers Dis. 2010; 20:1107–1118. [PubMed: 20413860]
34. Macbeth AH, Edds JS, Young WS III. Housing conditions and stimulus females: a robust social discrimination task for studying male rodent social recognition. Nat Protoc. 2009; 4:1574–1581. [PubMed: 19816420]
35. Madrigal JL, Feinstein DL, Dello RC. Norepinephrine protects cortical neurons against microglial-induced cell death. J Neurosci Res. 2005; 81:390–396. [PubMed: 15948176]
36. Madrigal JL, Leza JC, Polak P, Kalinin S, Feinstein DL. Astrocyte-derived MCP-1 mediates neuroprotective effects of noradrenaline. J Neurosci. 2009; 29:263–267. [PubMed: 19129402]
37. Maillet EL, Milon N, Heghinian MD, Fishback J, Schurer SC, Garamszegi N, et al. Noribogaine is a G-protein biased kappa-opioid receptor agonist. Neuropharmacology. 2015; 99:675–688. [PubMed: 26302653]
38. Markus T, Hansson SR, Cronberg T, Cilio C, Wieloch T, Ley D. beta-Adrenoceptor activation depresses brain inflammation and is neuroprotective in lipopolysaccharide-induced sensitization to oxygen-glucose deprivation in organotypic hippocampal slices. J Neuroinflammation. 2010; 7:94. [PubMed: 21172031]
39. Marsh SE, Abud EM, Lakatos A, Karimzadeh A, Yeung ST, Davtyan H, et al. The adaptive immune system restrains Alzheimer's disease pathogenesis by modulating microglial function. Proc Natl Acad Sci U S A. 2016; 113:E1316–E1325. [PubMed: 26884167]
40. Mather M, Harley CW. The Locus Coeruleus: Essential for Maintaining Cognitive Function and the Aging Brain. Trends Cogn Sci. 2016; 20:214–226. [PubMed: 26895736]
41. Matthews KL, Chen CP, Esiri MM, Keene J, Minger SL, Francis PT. Noradrenergic changes, aggressive behavior, and cognition in patients with dementia. Biol Psychiatry. 2002; 51:407–416. [PubMed: 11904135]
42. Modi KK, Jana A, Ghosh S, Watson R, Pahan K. A physically-modified saline suppresses neuronal apoptosis, attenuates tau phosphorylation and protects memory in an animal model of Alzheimer's disease. PLoS One. 2014; 9:e103606. [PubMed: 25089827]
43. Mori K, Ozaki E, Zhang B, Yang L, Yokoyama A, Takeda I, et al. Effects of norepinephrine on rat cultured microglial cells that express alpha1, alpha2, beta1 and beta2 adrenergic receptors. Neuropharmacology. 2002; 43:1026–1034. [PubMed: 12423672]
44. Murchison CF, Schutsky K, Jin SH, Thomas SA. Norepinephrine and ss(1)-adrenergic signaling facilitate activation of hippocampal CA1 pyramidal neurons during contextual memory retrieval. Neuroscience. 2011; 181:109–116. [PubMed: 21377513]
45. Murchison CF, Zhang XY, Zhang WP, Ouyang M, Lee A, Thomas SA. A distinct role for norepinephrine in memory retrieval. Cell. 2004; 117:131–143. [PubMed: 15066288]
46. Nguyen TV, Shen L, Vander GL, Quach LN, Belichenko NP, Saw N, et al. Small Molecule p75NTR Ligands Reduce Pathological Phosphorylation and Misfolding of Tau, Inflammatory

Changes, Cholinergic Degeneration, and Cognitive Deficits in AbetaPPL/S Transgenic Mice. J Alzheimers Dis. 2014

47. Oakley H, Cole SL, Logan S, Maus E, Shao P, Craft J, et al. Intraneuronal beta-amyloid aggregates, neurodegeneration, and neuron loss in transgenic mice with five familial Alzheimer's disease mutations: potential factors in amyloid plaque formation. J Neurosci. 2006; 26:10129–10140. [PubMed: 17021169]
48. Ohno M. Failures to reconsolidate memory in a mouse model of Alzheimer's disease. Neurobiol Learn Mem. 2009; 92:455–459. [PubMed: 19435612]
49. Paxinos, G., Franklin, KBJ. The Mouse Brain in Stereotaxic Coordinates. Academic Press; San Diego: 2001.
50. Pierce KL, Lefkowitz RJ. Classical and new roles of beta-arrestins in the regulation of G-protein-coupled receptors. Nat Rev Neurosci. 2001; 2:727–733. [PubMed: 11584310]
51. Qian L, Wu HM, Chen SH, Zhang D, Ali SF, Peterson L, et al. beta2-adrenergic receptor activation prevents rodent dopaminergic neurotoxicity by inhibiting microglia via a novel signaling pathway. J Immunol. 2011; 186:4443–4454. [PubMed: 21335487]
52. Rajagopal S, Rajagopal K, Lefkowitz RJ. Teaching old receptors new tricks: biasing seven-transmembrane receptors. Nat Rev Drug Discov. 2010; 9:373–386. [PubMed: 20431569]
53. Rezai-Zadeh K, Gate D, Gowing G, Town T. How to get from here to there: macrophage recruitment in Alzheimer's disease. Curr Alzheimer Res. 2011; 8:156–163. [PubMed: 21345166]
54. Rosenberg PB, Mielke MM, Tschanz J, Cook L, Corcoran C, Hayden KM, et al. Effects of cardiovascular medications on rate of functional decline in Alzheimer disease. Am J Geriatr Psychiatry. 2008; 16:883–892. [PubMed: 18978249]
55. Ross JA, McGonigle P, Van Bockstaele EJ. Locus Coeruleus, norepinephrine and Abeta peptides in Alzheimer's disease. Neurobiol Stress. 2015; 2:73–84. [PubMed: 26618188]
56. Ryan KJ, Griffin E, Yssel JD, Ryan KM, McNamee EN, Harkin A, et al. Stimulation of central beta2-adrenoceptors suppresses NFkappaB activity in rat brain: a role for IkappaB. Neurochem Int. 2013; 63:368–378. [PubMed: 23896303]
57. Samuels ER, Szabadi E. Functional neuroanatomy of the noradrenergic locus coeruleus: its roles in the regulation of arousal and autonomic function part I: principles of functional organisation. Curr Neuropharmacol. 2008; 6:235–253. [PubMed: 19506723]
58. Saul A, Sprenger F, Bayer TA, Wirths O. Accelerated tau pathology with synaptic and neuronal loss in a novel triple transgenic mouse model of Alzheimer's disease. Neurobiol Aging. 2013; 34:2564–2573. [PubMed: 23747045]
59. Savage JC, Jay T, Goduni E, Quigley C, Mariani MM, Malm T, et al. Nuclear receptors license phagocytosis by trem2+ myeloid cells in mouse models of Alzheimer's disease. J Neurosci. 2015; 35:6532–6543. [PubMed: 25904803]
60. Saxe MD, Battaglia F, Wang JW, Malleret G, David DJ, Monckton JE, et al. Ablation of hippocampal neurogenesis impairs contextual fear conditioning and synaptic plasticity in the dentate gyrus. Proc Natl Acad Sci U S A. 2006; 103:17501–17506. [PubMed: 17088541]
61. Schmittgen TD, Livak KJ. Analyzing real-time PCR data by the comparative C(T) method. Nat Protoc. 2008; 3:1101–1108. [PubMed: 18546601]
62. Schneider F, Baldauf K, Wetzel W, Reymann KG. Behavioral and EEG changes in male 5xFAD mice. Physiol Behav. 2014; 135:25–33. [PubMed: 24907698]
63. Schneider F, Baldauf K, Wetzel W, Reymann KG. Effects of methylphenidate on the behavior of male 5xFAD mice. Pharmacol Biochem Behav. 2015; 128:68–77. [PubMed: 25449360]
64. Schutsky K, Ouyang M, Castelino CB, Zhang L, Thomas SA. Stress and glucocorticoids impair memory retrieval via beta2-adrenergic, Gi/o-coupled suppression of cAMP signaling. J Neurosci. 2011a; 31:14172–14181. [PubMed: 21976502]
65. Schutsky K, Ouyang M, Thomas SA. Xamoterol impairs hippocampus-dependent emotional memory retrieval via Gi/o-coupled beta2-adrenergic signaling. Learn Mem. 2011b; 18:598–604. [PubMed: 21878527]
66. Schwartz M, Shechter R. Systemic inflammatory cells fight off neurodegenerative disease. Nat Rev Neurol. 2010; 6:405–410. [PubMed: 20531383]

67. Shimohama S, Taniguchi T, Fujiwara M, Kameyama M. Changes in beta-adrenergic receptor subtypes in Alzheimer-type dementia. J Neurochem. 1987; 48:1215–1221. [PubMed: 3029330]
68. Sil S, Ghosh T. Role of cox-2 mediated neuroinflammation on the neurodegeneration and cognitive impairments in colchicine induced rat model of Alzheimer's Disease. J Neuroimmunol. 2016; 291:115–124. [PubMed: 26857505]
69. Singhal G, Jaehne EJ, Corrigan F, Toben C, Baune BT. Inflammasomes in neuroinflammation and changes in brain function: a focused review. Front Neurosci. 2014; 8:315. [PubMed: 25339862]
70. Suryono, Kido J, Hayashi N, Kataoka M, Shinohara Y, Nagata T. Norepinephrine stimulates calprotectin expression in human monocytic cells. J Periodontal Res. 2006; 41:159–164. [PubMed: 16677282]
71. Tanaka KF, Kashima H, Suzuki H, Ono K, Sawada M. Existence of functional beta1- and beta2-adrenergic receptors on microglia. J Neurosci Res. 2002; 70:232–237. [PubMed: 12271472]
72. Tejani-Butt SM, Yang J, Zaffar H. Norepinephrine transporter sites are decreased in the locus coeruleus in Alzheimer's disease. Brain Res. 1993; 631:147–150. [PubMed: 8298987]
73. Thomas SA. Neuromodulatory signaling in hippocampus-dependent memory retrieval. Hippocampus. 2015; 25:415–431. [PubMed: 25475876]
74. Todd TP, Bucci DJ. Retrosplenial Cortex and Long-Term Memory: Molecules to Behavior. Neural Plast. 2015; 2015:414173. [PubMed: 26380115]
75. Violin JD, Lefkowitz RJ. Beta-arrestin-biased ligands at seven-transmembrane receptors. Trends Pharmacol Sci. 2007; 28:416–422. [PubMed: 17644195]
76. Yang JH, Lee EO, Kim SE, Suh YH, Chong YH. Norepinephrine differentially modulates the innate inflammatory response provoked by amyloid-beta peptide via action at beta-adrenoceptors and activation of cAMP/PKA pathway in human THP-1 macrophages. Exp Neurol. 2012; 236:199–206. [PubMed: 22609331]
77. Zhang J, Ferguson SS, Barak LS, Aber MJ, Giros B, Lefkowitz RJ, et al. Molecular mechanisms of G protein-coupled receptor signaling: role of G protein-coupled receptor kinases and arrestins in receptor desensitization and resensitization. Receptors Channels. 1997; 5:193–199. [PubMed: 9606723]

Reference List

1. Paxinos, G., Franklin, KBJ. The Mouse Brain in Stereotaxic Coordinates. Academic Press; San Diego: 2001.

Highlights

- Xamoterol is a highly selective ADRB1 partial agonist.
- Xamoterol has functional bias for cAMP versus β-arrestin signaling.
- Chronic xamoterol reduces pathology and neuroinflammation in 5XFAD model of AD.

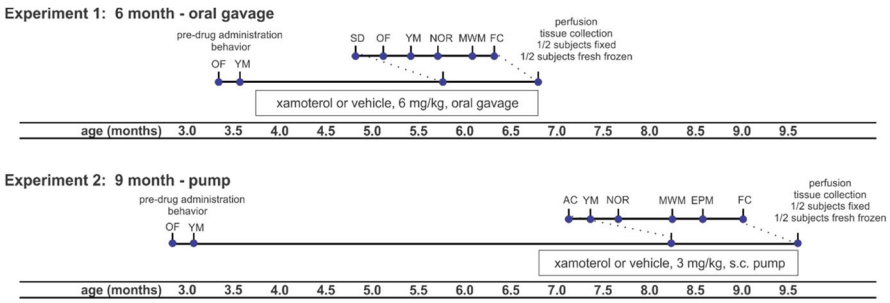

Fig. 1.

Timeline of *in vivo* studies indicates age, drug administration and behavioral testing schedules for Experiment 1 and Experiment 2. Two independent cohorts of 5XFAD and wildtype mice were chronically administered a selective partial ADRB1 agonist, xamoterol, or vehicle, 6 mg/kg oral gavage from 4.0 to 6.5 months of age or 3 mg/kg/day subcutaneous pump from 7.0 to 9.5 months of age. Experiment 1 is referred to as “6 month - oral gavage” as behavior and tissue collection occurs during the 6th month. Experiment 2 is likewise referred to as “9 month - pump”. Behavioral testing was performed in the indicated order during the final 4 to 5 weeks of administration. At the end of testing, mice were perfused and brains collected for neurobiochemical endpoints. Sample size = 10 to 11 per group for behavior and 4–6 per group for neurobiological endpoints. Experiments were analyzed independently. Abbreviations: OF, open field, AC, activity chamber; YM, Y-maze; SD, social discrimination; NOR, novel object recognition; MWM, Morris Water Maze; EPM, elevated plus maze; FC, fear conditioning; s.c., subcutaneous.

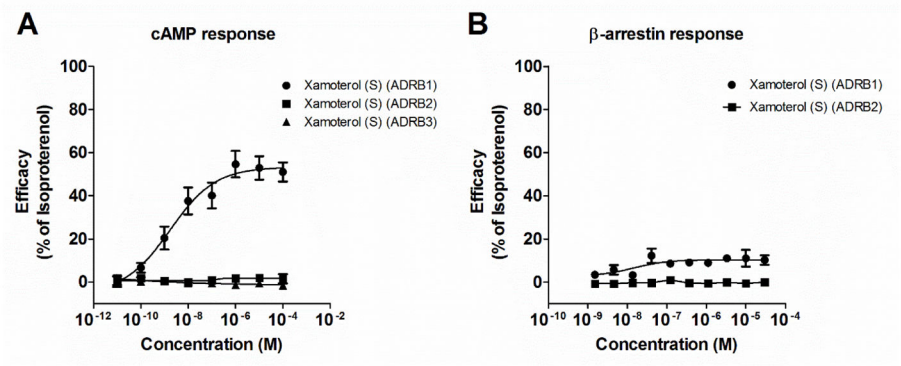

Fig. 2.

Xamoterol is a selective ADRB1 partial agonist with functional bias at the cAMP signaling pathway at the cloned human ADRB1 receptor. A) Dose-response curves for cAMP show xamoterol (S-enantiomer) with an efficacy of 50% relative to isoproterenol through the ADRB1 receptor and an EC_{50} of 2.2 nM (0.3–14.6 nM). Xamoterol has no cAMP activity through ADRB2 or ADRB3 up through 100 μM. B) Dose-response curves for β-arrestin activity show minimal (<10%) action of xamoterol on β-arrestin through ADRB1 or ADRB2. Data for cAMP represent 5 experiments performed in singlet or duplicate, and for β-arrestin, technical replicates within a single experiment.

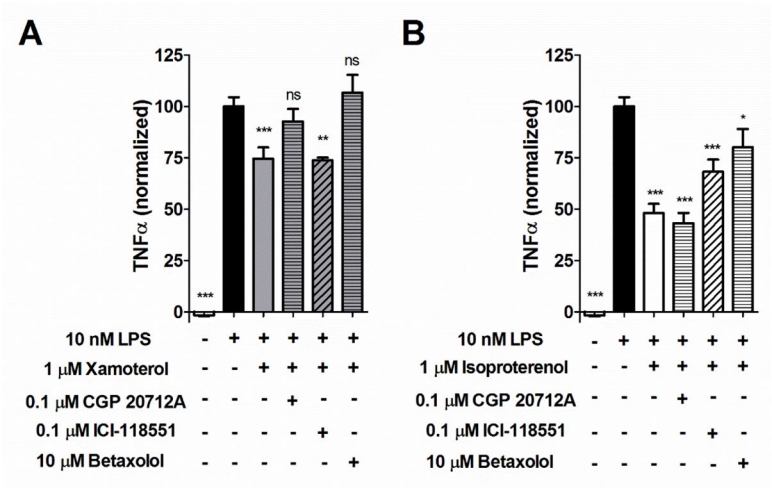

Fig. 3.

ADRB1 modulates LPS-induced TNF-α production in rat primary microglia. Both xamoterol (A; 1 μM), a selective partial agonist of the ADRB1 receptor, and isoproterenol (B; 1 μM), a non-selective full agonist of the ADRB1 receptor, reduced TNF-α production following challenge of primary rat microglia with LPS (10 ng/mL). A) Effects of xamoterol were reversed by pretreatment with either the selective ADRB1 antagonist, CGP 20712A (0.1 μM) or betaxolol (10 μM), but not the selective ADRB2 antagonist ICI-118551 (0.1 μM). B) Effects of isoproterenol, were partially reversed by pretreatment with the selective ADRB1 antagonist, betaxolol (10 μM) or the selective ADRB2 antagonist ICI-118551 (0.1 μM), but not CGP 20712A (0.1 μM). Data represent means ± SEM from multiple experiments (n= 4–9 per group) normalized to internal LPS controls. *p < .05, **p < .01, ***p < .001; ns, not significant; Dunnett's multiple comparisons against LPS exposure alone, following one-way ANOVA.

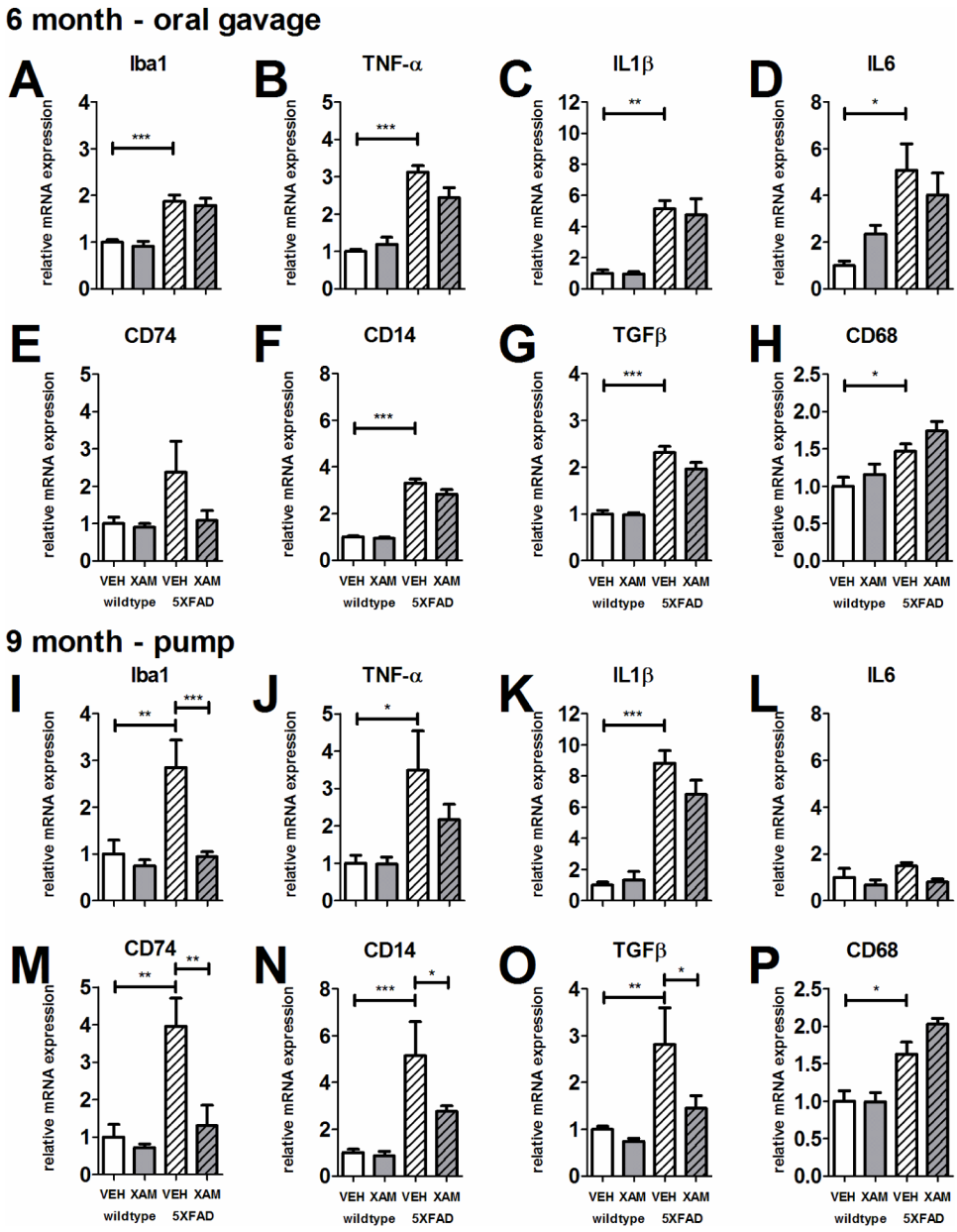

Fig. 4.

Xamoterol modulates immune-related mRNA expression in 5XFAD transgenic mice. Bar graphs depict mRNA expression in homogenized cortical tissue from wildtype and 5XFAD vehicle-treated and xamoterol-treated mice normalized relative to wildtype vehicle-treated mice for each gene (A–P). In the 6 month – oral gavage study (A–H), all genes with the exception of CD74 were elevated in vehicle-treated 5XFAD mice relative to wildtype counterparts. Likewise, in the 9 month – pump study (I–P), all genes with the exception of IL6 were elevated in vehicle-treated 5XFAD mice relative to wildtype. Xamoterol treatment attenuated Iba1, CD74, CD14 and TGFβ mRNA expression in 5XFAD mice (I,M–O) in the 9 month – pump study. In the 6 month – oral gavage study, trends for attenuation of TNF-α and CD14 were observed (B,F; $p < .1$). Sample size, n = 4–6 per group, but n=3 for 5XFAD-

VEH in 9 month – pump experiment. Data represent means +/− SEM. * $p < .05$, ** $p < .01$, *** $p < .001$, Bonferroni's test for multiple comparisons following one-way ANOVA.

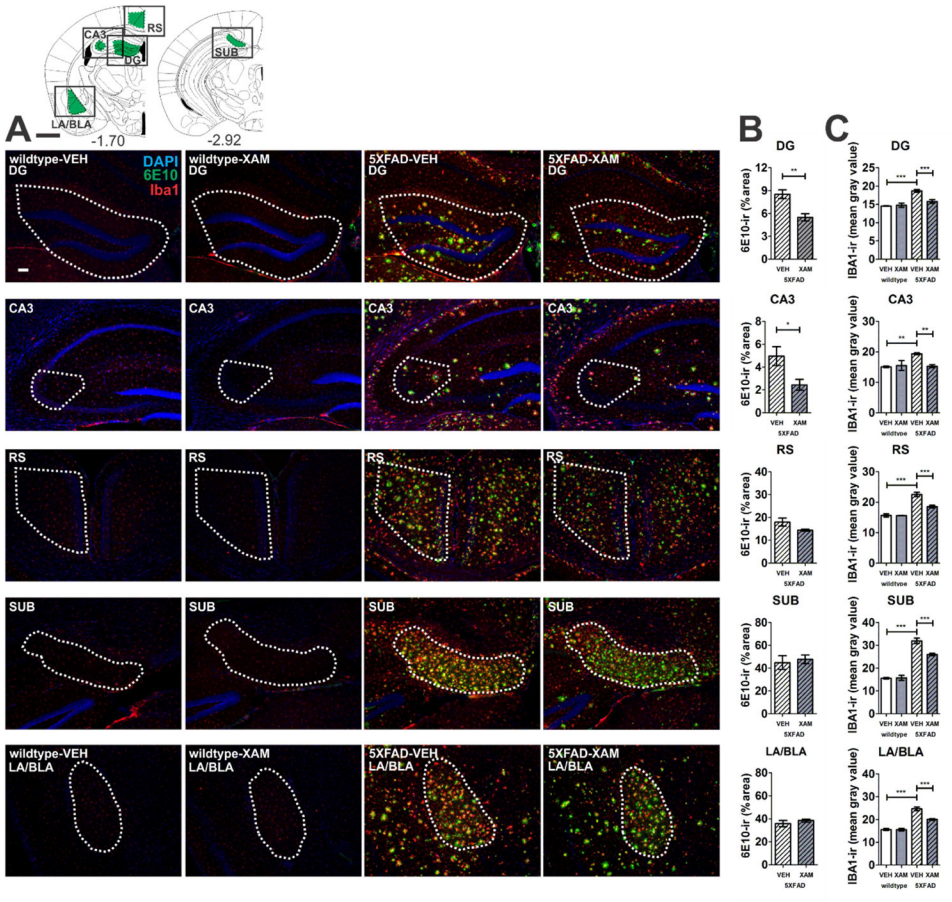

Fig. 5.

Xamoterol reduces microglia/macrophage (Iba1) gliosis and amyloid beta (6E10) immunoreactivity (-*ir*). Chronic dosing with the selective partial ADRB1 agonist, xamoterol, attenuates Iba1-*ir* in all regions in 5XFAD transgenic mice and reduces 6E10-*ir* in DG and CA3 regions of the hippocampus. A) Atlas plates (top left) indicate one of multiple levels from which the regions of interest (green) were selected for analyses [1]. Black boxes indicate image capture frame. Numbers below atlas plates indicate mm bregma; black scale bar, 1 mm. Photomicrographs (5X magnification) illustrate representative immunostaining (DAPI, blue; 6E10, green; Iba1, red) from each region of interest in wildtype and 5XFAD vehicle- (VEH) and xamoterol-treated (XAM) mice, white scale bar, 100 μm. Dashed white lines indicate region of quantification. B) Quantitative immunohistochemistry revealed decreases in 6E10-*ir* (% area) in DG and CA3. C) Increases in Iba1-*ir* (mean intensity) were detected in all regions analyzed in VEH-treated 5XFAD transgenic mice relative to VEH-treated wildtype littermates. These increases were attenuated in each region in transgenic mice chronically dosed with XAM. Sample size, n=4–5 per group, with exception of wildtype-XAM (n=3 for DG/CA3/SUB and n=2 for RS). Data represent mean ± SEM. *p < .05, **p < .01, ***p < .001, Bonferroni's test for multiple comparisons following one-way ANOVA. RS, retrosplenial cortex; LA/BLA, lateral/basolateral amygdala; SUB, subiculum; CA3, CA3 region of the hippocampus; DG, dentate gyrus.

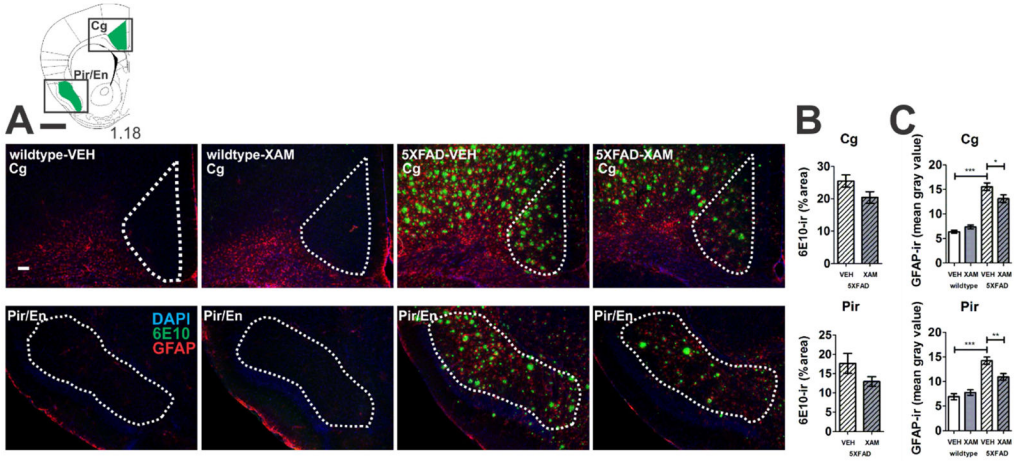

Fig. 6.

Xamoterol reduces astrocyte (GFAP) gliosis in the vicinity of amyloid beta (6E10) immunoreactivity (-*ir*). Chronic dosing with the selective partial ADRB1 agonist, xamoterol, attenuated GFAP-*ir* in the cingulate (Cg) and piriform/endopiriform (Pir/En) cortices in 5XFAD transgenic mice. A) Atlas plates (top left) indicate one of multiple levels from which the regions of interest (green) were selected for analyses [1]. Black boxes indicate image capture frame. Numbers below atlas plates indicate mm bregma; black scale bar, 1 mm. Photomicrographs (5X magnification) illustrate representative immunostaining (DAPI, blue; 6E10, green; GFAP, red) from each region of interest in wildtype and 5XFAD vehicle- (VEH) and xamoterol-treated (XAM) mice, white scale bar, 100 μm. Dashed white lines indicate region of quantification. B) Quantitative immunohistochemistry revealed non-significant trends for decreases in 6E10-*ir* (% area) in Cg and Pir/En. C) Increases in GFAP-*ir* (mean intensity) were detected in both Cg and Pir/En in VEH-treated 5XFAD transgenic mice relative to VEH-treated wildtype littermates. These increases in astrogliosis were attenuated in both regions in transgenic mice chronically dosed with XAM. Sample size, n=4–5 per group. *p < .05, **p < .01, ***p < .001, Bonferroni's test for multiple comparisons following one-way ANOVA.

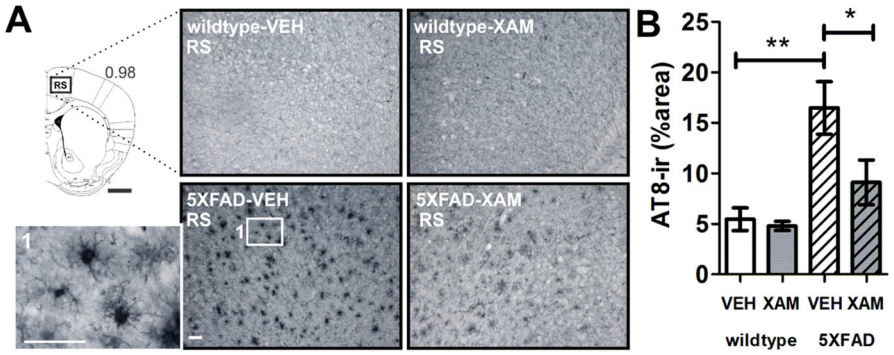

Fig. 7.

Chronic dosing with the selective partial ADRB1 agonist, xamoterol, attenuated AT8-*ir* in the retrosplenial cortex (RS) in 5XFAD transgenic mice. A) Atlas plate indicates the level at which images were selected for analyses [1]. Black box indicates image capture frame. Number below atlas plate indicates mm bregma; black scale bar, 1 mm. Photomicrographs (10X magnification) illustrate representative AT8-immunostaining in wildtype and 5XFAD vehicle- (VEH) and xamoterol-treated (XAM) mice, white scale bar, 50 μm. B) Quantitative immunohistochemistry revealed increases in AT8-*ir* (% area) in VEH-treated 5XFAD transgenic mice relative to VEH-treated wildtype littermates. These increases were attenuated in transgenic mice chronically dosed with XAM. Sample size, n=5 per group. *p < .05, **p < .01, Bonferroni's test for multiple comparisons following one-way ANOVA.

Table 1

Select genes for mRNA expression related to neuroinflammation.

Gene	Name	Description
Iba1	ionized calcium-binding adapter molecule 1	constitutively expressed by microglia and macrophages
TNFα	tumor necrosis factor alpha	proinflammatory cytokine
IL1β	interleukin 1 beta	proinflammatory cytokine
IL6	interleukin 6	proinflammatory cytokine
CD74	cluster of differentiation 74	class II histocompatibility complex antigen binding
CD14	cluster of differentiation 14	antigen detection
TGFβ	transforming growth factor beta	modulator of immune cell proliferation
CD68	cluster of differentiation 68; macrosialin	scavenger receptor family member related to phagocytosis; lysosomal in activated macrophages and microglia

Table 2

5XFAD behavior: 6 month – oral gavage study.

Behavior	age (mon.)	wildtype – vehicle	wildtype - xamoterol	5XFAD - vehicle	5XFAD – xamoterol	Statistics
pre-dose Open Field (distance moved, cm)	*3.4*	6232.6 ± 323.2	6179.9 ± 288.8	5767.4 ± 355.7	7131.3 ± 437.9	one-way ANOVA NS
pre-dose Y-Maze (% alternation)	*3.5*	54.6 ± 3.5	**57.4 ± 1.8	*56.1 ± 2.3	55.2 ± 4.4	one sample t-tests versus chance (50%); * **p < .05,** ** **p < .01**
Social Discrimination (discrimination ratio)	*5.4*	0.034 ± 0.152	0.137 ± 0.098	0.270 ± 0.071	0.109 ± 0.132	one-way ANOVA NS
Open Field (distance moved, cm)	*5.5*	7458.0 ± 559.5	6434.4 ± 397.7	7319.6 ± 553.9	7875.5 ± 815.0	one-way ANOVA NS
Y-Maze (% alternation)	*5.6*	50.7 ± 3.7	56.4 ± 3.2	***64.3 ± 2.9	53.0 ± 4.2	one sample t-tests versus chance (50%) *** **p < .001**
NOR (discrimination ratio)	*5.8*	0.391 ± 0.091	0.446 ± 0.037	0.278 ± 0.086	0.551 ± 0.039	one-way ANOVA $F_{(3,36)}$ = 2.794; p = .054; TREND
Morris Water Maze (escape latency; sec)	*6.2*					two-way ANOVA
day 1		58.2 ± 0.9	55.5 ± 1.9	57.9 ± 1.2	50.7 ± 3.2	DAY: $F_{(5,31)}$ = 29.31 ***p < 0.001
day 2		49.7 ± 4.4	47.4 ± 3.7	44.9 ± 4.0	45.1 ± 2.7	GROUP: NS INTERACTION: NS
day 3		39.0 ± 3.7	44.9 ± 4.0	42.7 ± 4.5	30.3 ± 3.8	
day 4		40.9 ± 7.7	43.1 ± 4.3	41.7 ± 4.9	30.3 ± 4.0	
day 5		27.6 ± 8.1	35.0 ± 4.2	35.0 ± 4.9	30.5 ± 4.1	
day 6		25.9 ± 4.9	28.7 ± 4.6	34.8 ± 5.5	23.1 ± 4.1	
MWM - probe trial (target quadrant ratio)		0.99 ± 0.20	1.06 ± 0.13	1.03 ± 0.19	*1.43 ± 0.10	one sample t-tests * ratio > 1.0; * **p < .05**

Table 3

5XFAD behavior: 9 month – pump study.

Behavior	age (mon.)	wildtype – vehicle	wildtype - xamoterol	5XFAD - vehicle	5XFAD – xamoterol	Statistics
pre-dose Open Field (distance moved, cm)	*3.1*	6686.8 ± 279.1	6502.9 ± 176.4	6208.2 ± 719.8	6886.7 ± 374.3	one-way ANOVA NS
pre-dose Y-Maze (% alternation)	*3.2*	54.4 ± 2.7	53.8 ± 2.3	*57.2 ± 2.7	*57.8 ± 2.7	one sample t-tests versus chance (50%); * **p < .05**
Activity Chamber (distance moved, cm)	*8.0*	4418.7 ± 564.8	5192.5 ± 385.9	5053.3 ± 571.0	4487.6 ± 300.7	one-way ANOVA NS
Y-Maze (% alternation)	*8.1*	53.6 ± 2.3	*58.8 ± 3.0	*57.8 ± 2.7	*55.8 ± 2.2	one sample t-tests versus chance (50%); * **p < .05**
NOR (discrimination ratio)	*8.4*	0.239 ± 0.052	0.158 ± 0.043	0.159 ± 0.066	0.305 ± 0.066	one-way ANOVA NS
Morris Water Maze (escape latency; sec)	*8.8*					two-way ANOVA
day 1		52.0 ± 3.6	36.7 ± 4.0	50.1 ± 3.3	51.6 ± 3.3	DAY: $F_{(3,30)}$ = 44.84 ***p < 0.001
day 2		29.9 ± 4.0	28.4 ± 6.8	40.3 ± 4.0	33.4 ± 4.9	GROUP: $F_{(3,30)}$ = 2.612; p = .060; TREND
day 3		36.1 ± 4.1	19.9 ± 5.6	29.0 ± 4.0	20.7 ± 3.4	INTERACTION: $F_{(9,30)}$ = 1.982 p = .051; TREND
day 4		29.9 ± 4.5	16.6 ± 4.1	19.4 ± 2.8	17.0 ± 2.2	
MWM - probe trial (target quadrant ratio)		2.60 ± 0.74	*5.00 ± 1.46	*6.07 ± 1.30	*4.24 ± 0.94	one sample t-tests * ratio > 1.0; * **p < .05**
Elevated Plus Maze (% time open arms)	*9.1*	9.9 ± 2.6	7.5 ± 1.4	18.2 ± 5.2	11.1 ± 2.9	one-way ANOVA NS
Fear Conditioning						one-way ANOVA
Acquisition (% freezing – trace)	*9.3*	34.7 ± 7.6	57.5 ± 7.9	37.1 ± 7.9	42.5 ± 5.9	NS
Cued Recall (% freezing – trace)	*9.3*	30.3 ± 7.2	20.2 ± 5.8	29.4 ± 7.3	33.6 ± 4.3	NS
Contextual Recall (% freezing min 2–5)	*9.3*	27.1 ± 7.5	32.1 ± 9.1	19.8 ± 4.7	16.8 ± 3.1	NS